

Detection of residual native state entropy changes
upon mutation in Fyn SH3

Kresten Lindorff-Larsen^{1,2,3}, Robert B. Best^{1,4}, Anthony Mittermaier^{5,6},
Lewis E. Kay^{5,7}, Christopher M. Dobson^{1,8}, and Michele Vendruscolo^{1,*}

¹Department of Chemistry, University of Cambridge, Lensfield Road,
Cambridge, CB2 1EW, United Kingdom

²Department of Biochemistry, Institute of Molecular Biology and Phys-
iology, University of Copenhagen, Universitetsparken 13, DK-2100 Copen-
hagen Ø, Denmark

³Current address: Structural Biology and NMR Laboratory & the Linderstrøm-
Lang Centre for Protein Science, Department of Biology, University of Copen-
hagen, 2200 Copenhagen, Denmark

⁴Laboratory of Chemical Physics, NIDDK, National Institutes of Health,
Bethesda, Maryland 20892-0520, U.S.A.

⁵Department of Biochemistry, University of Toronto, Toronto, Ontario,
Canada M5S 1A8

⁶Current address: Department of Chemistry, McGill University, 801
Sherbrooke St. W., Montreal, QC H3A 0B8, Canada

⁷Departments of Medical Genetics and Chemistry, University of Toronto,
Toronto, Ontario, Canada M5S 1A8

⁸Deceased

*Corresponding author. Email: mv245@cam.ac.uk

Abstract¹

NMR relaxation experiments have shown that there are small but measurable changes in the native state dynamics of the Fyn SH3 domain associated with the substitution by other amino acids of a phenylalanine residue (F20) in the hydrophobic core. We have here used experimental values of NMR order parameters for the wild type protein and two mutational variants (F20L and F20V) as restraints in molecular dynamics simulations. This approach is highly sensitive and provides an atomistic description of the subtle perturbations in native state fluctuations accompanying the mutations. The structural ensembles that we have determined using this method allow the changes in the native state entropy of the protein caused by each of the mutations to be estimated. These entropy changes correspond to free energy variations of several kcal mol⁻¹ and therefore represent sizable contributions to the overall changes in stability that are associated with the amino acid mutations.

Keywords: Entropy/Mutation/NMR relaxation/Protein dynamics/Protein stability

¹This manuscript was written in Cambridge, Toronto and Copenhagen in 2004–2005, forms part of K.L.-L.’s PhD thesis (Lindorff-Larsen 2004), and was uploaded to arXiv in 2026.

Introduction

Natural mutations in proteins are at the heart of molecular evolution (Graur & Li 2000), and are the origins of many familial diseases (Dobson 2003). In the laboratory, the introduction of specific mutations through the technique of protein engineering represents a powerful approach that can be used to perturb in a controlled manner a wide range of properties of a protein. Consequently, the effects of amino acid mutations on function (Leatherbarrow & Fersht 1986; Brannigan & Wilkinson 2002), structure (Eriksson *et al.* 1992; Baldwin *et al.* 1993; Buckle *et al.* 1993), stability (Serrano & Fersht 1989; Serrano *et al.* 1992; Carter *et al.* 2001; Gromiha *et al.* 2002; Guerois *et al.* 2002; Kortemme & Baker 2002; Bordner & Abagyan 2004; Capriotti *et al.* 2005), folding (Evans *et al.* 1987; Matouschek *et al.* 1989; Fersht *et al.* 1992) and aggregation (Chiti *et al.* 2000, 2002, 2003; de la Paz & Serrano 2004; DuBay *et al.* 2004; Pawar *et al.* 2005) have been the focus of much research.

The dynamical aspects of proteins are now recognized as playing a central role in their function (McCammon & Wolynes 1977; Frauenfelder *et al.* 1991; Rasmussen *et al.* 1992; Eisenmesser *et al.* 2002; Karplus & McCammon 2002; Wong & McCammon 2003; Benkovic & Hammes-Schiffer 2003). Further, protein dynamics is intimately linked to the thermodynamics of protein stability and ligand affinity (Cooper 1976; Akke *et al.* 1993; Yang & Kay 1996; Li *et al.* 1996; Zidek *et al.* 1999; Wrabl *et al.* 2000; Mittermaier & Kay 2004; Spyropoulos 2005). Protein engineering methods have the possibility to provide unique insights into the determinants of protein mobility, and recently the details of the changes in native state dynamics that occur upon amino acid mutations have been the subject of a variety of experimental studies (Stone 2001; Stone *et al.* 2001; Mayer *et al.* 2003; Millet *et al.* 2003; Mittermaier & Kay 2004).

In this paper we describe an approach to perform a structural analysis of the ensembles of protein conformations that are populated in the native state

and to determine thermodynamic consequences of the changes in native state dynamics that accompany amino acid substitutions. In the technique that we use, data from heteronuclear NMR relaxation experiments are combined with computer simulations in order to describe native state heterogeneity. In particular, experimentally derived backbone and side-chain order parameters for the Fyn SH3 domain and two hydrophobic core mutants (F20L and F20V) (Mittermaier & Kay 2004) are used as restraints in molecular dynamics (MD) simulations (Best & Vendruscolo 2004; Lindorff-Larsen *et al.* 2005). In these simulations a molecular mechanics force-field is used as a motional model to interpret experimental NMR relaxation data for the two mutants, and thus to provide a structural description of the changes in native state heterogeneity associated with the alteration of the fluctuations that occur upon amino acid substitution. Our results show that both mutations cause small, but measurable, changes in such heterogeneity. Although the native states of the F20L and F20V mutational variants are destabilized relative to the unfolded state in terms of the total free energy, the increased internal mobility caused by the two mutations corresponds to an entropic stabilization of the native state of several kcal mol⁻¹. This observation has important implications for the interpretation of protein engineering data and for understanding the factors that control protein stability.

Methods

Molecular dynamics simulations

Molecular dynamics simulations of chicken Fyn SH3 and two of its mutational variants (F20L and F20V) were performed using CHARMM (Brooks *et al.* 1983). The structure of chicken Fyn SH3 has not been determined experimentally but is known to be very similar to that of the human variant (Mittermaier & Kay 2004). Therefore, a model of the structure of the

chicken isoform, herein termed Fyn SH3, was generated by introducing the two mutations V1S and V5E into the structure of the human isoform (PDB entry 1SHF) using Deep-View (Schwede *et al.* 2003) and subsequently energy minimizing the resulting structure. Also, the two mutants of Fyn SH3, F20L and F20V, are known to have a virtually identical backbone structure to that of the wild-type (WT) protein (Mittermaier & Kay 2004); these two mutations were therefore modelled in a similar manner. Simulations were carried out using a polar hydrogen model and Param19 force-field (Neria *et al.* 1996). The effects of water were modelled by surrounding the proteins by a 5Å solvation shell consisting of 724 TIP3P water molecules (Jorgensen *et al.* 1983); a boundary potential was used to prevent water molecules from escaping (Beglov & Roux 1995). All simulations were carried out at 298 K.

Experimentally determined squared order parameters (S^2 values) were used as restraints (Best & Vendruscolo 2004). In this type of simulations a set of molecules is simulated in parallel since the order parameter for a single molecule at any given time is by definition unity. It has previously been shown that simulations using 8, 16 or 32 molecules (replicas) provide very similar and well converged results (Best & Vendruscolo 2004). All simulations reported here were obtained by simulating an ensemble consisting of $N_{rep} = 16$ replicas of the protein.

At each step of the MD simulations S^2 values were calculated across this ensemble using (Henry & Szabo 1985; Best & Vendruscolo 2004)

$$S_{ij}^2 = \frac{3}{2}(\langle \hat{x}_{ij}^2 \rangle^2 + \langle \hat{y}_{ij}^2 \rangle^2 + \langle \hat{z}_{ij}^2 \rangle^2 + 2\langle \hat{x}_{ij}\hat{y}_{ij} \rangle^2 + 2\langle \hat{x}_{ij}\hat{z}_{ij} \rangle^2 + 2\langle \hat{y}_{ij}\hat{z}_{ij} \rangle^2) - \frac{1}{2} \quad (1)$$

where S_{ij}^2 is the calculated squared order parameter between atoms i and j , and \hat{x}_{ij} , \hat{y}_{ij} and \hat{z}_{ij} are the components of a unit vector along this bond. The resulting S_{calc}^2 were then compared to the N experimentally determined values according to

$$\rho(t) = \frac{1}{N} \sum_{k=1}^N (S_{k,calc}^2(t) - S_{k,exp}^2)^2 \quad (2)$$

The value of $\rho(t)$ therefore measures the mean square deviation between experimental and calculated S^2 values. During the simulations ρ was progressively decreased by performing biased MD using the energetic penalty (Paci & Karplus 1999; Best & Vendruscolo 2004)

$$E(\rho(t)) = \begin{cases} \frac{\alpha N_{rep}}{2}(\rho(t) - \rho_0(t))^2 & \text{if } \rho(t) > \rho_0(t) \\ 0 & \text{if } \rho(t) \leq \rho_0(t) \end{cases} \quad (3)$$

where α is a force-constant that determines the weight of the S^2 restraints relative to the molecular mechanics force field, and $\rho_0(t)$ is defined as

$$\rho_0(t) = \min_{0 \leq \tau \leq t} \rho(\tau) \quad (4)$$

The simulations were initiated with a 200 ps heating phase with $\alpha = 10^3 \text{ kcal mol}^{-1}$. Then, over a simulation period of 140 ps, α was progressively increased to $1.6 \cdot 10^7 \text{ kcal mol}^{-1}$. Finally a 1.0 ns production phase ($\alpha = 1.0 \cdot 10^7 \text{ kcal mol}^{-1}$) was used to sample the native state variability of Fyn SH3 and the two mutational variants. The convergence of these simulations was estimated by splitting the simulation up into four equally sized parts and analysing each separately. The quasiharmonic analysis of the configurational entropy (see below) revealed that fully converged values could be obtained from the last half of the simulations. Thus, by saving structures every 10 ps we obtained ensembles consisting of 800 structures (50 from the last 500ps for each replica) for each of the three proteins.

A total of 44 (17), 48 (22) and 44 (19) amide (methyl) S^2 restraints were used for WT, F20L and F20V, respectively, after discarding experimental S^2 values that may contain contributions from slower motions on the ns timescale (amide groups of E5, S31, S32, E33, G34, A39 and methyl groups of L42, V58) (Mittermaier & Kay 2004). All data were obtained at 298 K, the same temperature as that used in the simulations.

Quasi-harmonic analysis

A quasi-harmonic analysis (Karplus & Kushick 1981; Levy *et al.* 1984; Case 1994; Brooks *et al.* 1995) was performed in CHARMM. The vibrational contribution to the native state entropy (S_{vib}) was estimated from the frequencies obtained (Karplus & Kushick 1981; Levy *et al.* 1984; Brooks *et al.* 1995; McQuarrie 2000). Before the analysis all water molecules and hydrogen atoms were removed. Reported numbers correspond to $T\Delta S_{vib}$. Error estimates of S_{vib} were obtained by a bootstrap procedure (Efron & Tibshirani 1986). One hundred ensembles, each containing 800 structures, were sampled (with replacement) from the original ensemble, and each ensemble was subsequently used as input to a quasiharmonic analysis. The reported error bounds are the standard deviations across these 100 ensembles. As noted above, convergence was evaluated by analysing the total simulation in equally sized blocks, and the values reported are fully converged within the error bounds shown.

Results

Ensembles representing the native state dynamics

Order parameters (S^2 values) derived from NMR relaxation experiments provide a high resolution measure of the amplitudes of motions in proteins (Kay 1998, 2005). Thus, despite the fact that the ns timescale fluctuations in WT Fyn SH3 and in the two mutants (F20L and F20V) are very similar, the experimental data can be obtained with sufficient accuracy (Millet *et al.* 2002) to detect small local differences (Mittermaier & Kay 2004). If these subtle differences are to be interpreted in structural terms, it is therefore crucial that the structural models reproduce the experimental data with high precision. It is extremely difficult to obtain this level of accuracy by a direct integration of the equation of motions using conventional force-fields (Best

et al. 2004). We therefore carried out a series of MD simulations in which the experimental amide and side-chain S^2 values were used directly as restraints (Best & Vendruscolo 2004; Lindorff-Larsen *et al.* 2005), thereby introducing the experimentally observed variability into the structural ensembles (Figure 1). The agreement between experimental and calculated S^2 values is shown in Figure 2A; the correlations and root mean square deviations (RMSDs) between the two sets of S^2 values are $r^2 = 0.93$ (RMSD = 0.038), 0.96 (0.043) and 0.91 (0.043) for WT, F20L and F20V, respectively, showing the very good agreement that can be obtained between the experimental and predicted S^2 values when the latter are imposed as restraints. Nevertheless, despite these high correlations, it remains important to examine the level to which the changes in S^2 values between the WT and mutant proteins are reproduced by the calculated structures (Figure 2B). There is a very good agreement, with correlations and RMSDs between experimental and calculated values of $\Delta(S^2)$ of $r^2 = 0.79$ and RMSD = 0.020 for F20L and $r^2 = 0.71$ and RMSD = 0.025 for F20V. The q -factors, defined as $q = \sqrt{\sum(\Delta S_{calc}^2 - \Delta S_{exp}^2)^2} / \sqrt{\sum(\Delta S_{calc}^2)^2}$, are 0.51 for both F20L and F20V.

Given this high level of agreement between experimental and calculated S^2 values, it becomes possible to provide a detailed analysis of the motions associated with the observed order parameters and their changes upon mutation. As an example, we show the distribution of ten side-chain dihedral angles in the WT and mutant proteins (Figure 3). It is clear that the molecular motion giving rise to $S^2 < 1$ can include contributions from both variability within a single energy well (e.g. ‘diffusion in a cone’-type motion (Kay 1998)) and from transitions between wells (rotameric transitions). No simple motional models will therefore be able to describe well the overall fluctuations in the structure. The high similarity between the dihedral angle distributions obtained for the WT and mutant proteins is a consequence

of the very similar experimental S^2 values for the three variants, and in addition shows that the MD simulations have converged well. These results indicate that the experimental changes in side-chain S^2 values result mainly from subtle shifts in the populations of side-chain rotamers associated with the amino acid substitutions at position 20 in the Fyn SH3 domain.

Mutational changes to the residual native state entropy

It has been suggested that the mobility probed by experimental S^2 values is associated with significant entropy contributions (Akke *et al.* 1993; Yang & Kay 1996; Li *et al.* 1996; Wrabl *et al.* 2000; Spyropoulos 2005). A quantitative analysis of this effect is complicated by the theoretical and practical difficulties in estimating absolute values of entropies. Nevertheless, using a range of motional models for amide and methyl groups, an analytic relationship has been derived relating changes in order parameters to entropy changes (Yang & Kay 1996). Based on this method and the experimental amide and methyl S^2 values in Fyn SH3 it has been estimated that the F20L and F20V mutations are accompanied by an entropic stabilization ($T\Delta S_{vib}$) of the native state by 1.95 and 3.82 kcal mol⁻¹, respectively (Mittermaier & Kay 2004). Notably, these values are comparable in magnitude to the free energy of unfolding of the WT Fyn SH3 domain (-2.4 kcal mol⁻¹) (Northey *et al.* 2002). Overall, however, the F20L and F20V mutations destabilize the protein relative to WT Fyn SH3 by 1.1 and 1.9 kcal mol⁻¹, respectively (Northey *et al.* 2002). These estimates of the entropic contributions to stability changes represent, therefore, a large fraction of the net free energy of the native protein relative to its denatured state. As the values for the entropy terms are based on simplified models for the motion associated with the experimental S^2 values, it is important to validate them by alternative methods of analysis. In addition, these estimates are based on the assumption that the overall entropy can be obtained as the sum of individual

contributions, which is strictly valid only if all intramolecular motions are independent of each other; for correlated motions, this assumption will lead to overestimates of the entropic contributions to the native state stability.

In the light of these considerations, we performed a quasi-harmonic analysis (Brooks *et al.* 1995) of the structural ensembles obtained in this study to determine the density of states of vibrational modes in the three variants (Figure 4A). The analysis was carried out for the side chains for which experimental order parameters were available in all three proteins as well as for the polypeptide backbone. The results show that both F20L and F20V display more extensive low frequency motions than the WT protein, in particular in the range $\nu = 50\text{--}1000\text{ ns}^{-1}$. From the frequencies involved it is possible to estimate the vibrational contribution to the native state entropy (Karplus & Kushick 1981; Levy *et al.* 1984; Brooks *et al.* 1995). The results are shown in Figure 4B and show that the changes in vibrational entropy upon mutation correspond to large changes in free energy ($T\Delta S_{vib}$). Using, for example, the first 250 modes we obtain estimates of 7.8 ± 0.8 and $7.9 \pm 0.7\text{kcal mol}^{-1}$ for F20L and F20V, respectively.

Discussion

Protein engineering is an important method of modulating protein stability and many studies have focused on the rationalization and prediction of changes in the native state stability accompanying amino acid substitutions (Serrano *et al.* 1992; Doig & Sternberg 1995; Carter *et al.* 2001; Gromiha *et al.* 2002; Guerois *et al.* 2002; Kortemme & Baker 2002; Bordner & Abagyan 2004). These methods are based on the assumption that the changes in stability resulting from a mutation can be related to changes in intramolecular interaction energies and solvation energies, and in the configurational entropy of the unfolded protein; changes in the residual native state entropy are often assumed to be negligible. NMR relaxation measure-

ments, however, provide evidence that there are often measurable changes in native state dynamics associated with mutations (Stone *et al.* 2001; Millet *et al.* 2003; Mayer *et al.* 2003; Mittermaier & Kay 2004; Goehlert *et al.* 2005). Moreover, it has been suggested that these changes, although small, may correspond to entropy differences that, when converted into free energies, are of the same order of same magnitude as the changes in native state stability. Further, it has recently been suggested that arginine to lysine mutations may entropically stabilize the native state of hyperthermophilic proteins (Berezovsky *et al.* 2005). Consequently, these changes in native state entropy may be important factors to be considered in order to understand and to predict stability changes upon mutation. A detailed analysis of the basis for these changes is therefore of considerable significance.

Previous estimates of the free energy changes from order parameters have made two assumptions about the relationship between measured order parameters and native state entropies: (i) that the re-orientations of individual atomic bond vectors are independent of each other, and (ii) that the motions involved can be described by models that are sufficiently simple that an analytical relationship can be derived between order parameters and entropies. Although both computational and experimental studies (Yang & Kay 1996; Prompers & Brüschweiler 2000; Stone *et al.* 2001; Lee *et al.* 2002; Mayer *et al.* 2003) suggest that these approximations are relatively good, in particular when calculating entropy changes, it still remains important to test their validity. The method of analysing changes in native state entropy that we have here presented does not require these approximations. The use of MD simulations restrained by S^2 values enables us to replace the analytical models (e.g. that described as ‘diffusion in a cone’) with a procedure in which the underlying CHARMM molecular mechanics force-field is used to generate a detailed description of the possible intramolecular motions. Using this procedure we find that the experimental changes in order param-

eters in the F20L and F20V variants of Fyn SH3 translate into free energy changes on the order of several kcal mol⁻¹. These values are of the same order of magnitude as the stability changes that accompany these mutations and therefore constitute an important term in the overall effect on stability.

The procedure that we have used for estimating entropy changes is based on a set of assumptions that differs from those discussed above and include the use of (i) restrained MD simulations to sample the conformational space, and (ii) a quasi-harmonic approximation to describe the molecular motions. Since these assumptions are different from those in the semi-analytical approach, it is highly encouraging that the two methods give estimates of entropy changes of the same sign and magnitude. A more detailed analysis will require the development of methods for estimating entropies from structural ensembles that take anharmonic contributions more fully into account (Cheluvareja & Meirovitch 2005). Finally, both procedures used to relate the entropy changes to the variations in the free energy of unfolding assume that the changes in vibrational entropy of the unfolded state are negligible. This assumption may hold for a highly denatured state in which specific contacts are absent, although in some proteins amino acid mutations are known to cause long range changes in the structure and dynamics of the unfolded state (Klein-Seetharaman *et al.* 2002; Fieber *et al.* 2004). The thermodynamic consequences of such changes is, however, difficult to estimate due to the theoretical problems in relating relaxation experiments for disordered systems to structural features and due to sampling problems for unfolded proteins in molecular dynamics simulations.

Proteins are stabilized by a multitude of weak interactions, and protein structures can be considered at least partially liquid-like (Zhou *et al.* 1999; Lindorff-Larsen *et al.* 2005; Best *et al.* 2005). In such systems the removal or weakening of stabilizing interactions is expected to cause an increase in the fluctuations in the remainder of the system, and hence to increase its con-

figurational entropy (Dunitz 1995; Qian 1998). Experimentally, this effect has been difficult to observe in relation to protein engineering experiments. This is partially due to technical issues pertaining to the methods by which entropy and enthalpy is measured (Beasley *et al.* 2002), as well as the large solvent contributions to thermodynamic parameters (Vaughan *et al.* 1999). The procedure that we here describe allows for a direct and quantitative determination of changes in the configurational entropy of proteins, and thus provides a crucial tool to understand the complicated interplay between stabilizing interactions and molecular fluctuations.

The observation that the experimentally observed decrease in stability of the native states of the F20L and F20V mutant proteins may include large contributions from changes in native state configurational entropy that oppose a loss in enthalpy has important consequences for the understanding and use of the protein engineering method to modulate stabilities. Thus, models that rationalize the stability change of mutant proteins in terms of changes in intramolecular contacts and solvation energies should also include changes in the residual entropy of the native states.

Finally, the increasing availability of experimental measurements of backbone and side-chain dynamics is making it possible to predict order parameters from protein structures with reasonable accuracy (Goodman *et al.* 2000; Zhang & Brüschweiler 2002; Ming & Brüschweiler 2004). If these types of procedures become sufficiently accurate to enable reliable predictions to be made of the changes in order parameters from mutations it should be possible to calculate the corresponding changes in residual entropies using the approach described here without the need of experimental measurements. The resulting values can then be used as an integral part of design procedures that attempt to modulate protein stability by means of amino acid substitutions.

Acknowledgments

KLL was supported by the Danish Research Agency and an EMBO long-term fellowship. LEK acknowledges support from the Canadian Institutes of Health Research. LEK holds a Canada Research Chair in Biochemistry. MV is a Royal Society University Research Fellow. The research of CMD and MV is supported in part by Programme Grants from the Wellcome and Leverhulme Trusts.

References

- Akke, M., Brüschweiler, R., & Palmer, A. G. (1993). *J. Am. Chem. Soc.* **115**, 9832–9833.
- Baldwin, E. P., Hajiseyedjavadi, O., Baase, W. A., & Matthews, B. W. (1993). *Science*, **263**, 1715–1718.
- Beasley, J. R., Doyle, D. F., Chen, L., Cohen, D. S., Fine, B. R., & Pielak, G. J. (2002). *Proteins*, **49**, 398–402.
- Beglov, D. & Roux, B. (1995). *Biopolymers*, **35**, 171–178.
- Benkovic, S. J. & Hammes-Schiffer, S. (2003). *Science*, **301**, 1196–1202.
- Berezovsky, I., Chen, W., Choi, P., & Shakhnovich, E. (2005). *PLoS Comput. Biol.* **in press**.
- Best, R. B., Clarke, J., & Karplus, M. (2004). *J. Am. Chem. Soc.* **126**, 7734–7735.
- Best, R. B., Clarke, J., & Karplus, M. (2005). *J. Mol. Biol.* **349**, 185–203.
- Best, R. B. & Vendruscolo, M. (2004). *J. Am. Chem. Soc.* **126**, 8090–8091.
- Bordner, A. J. & Abagyan, R. A. (2004). *Proteins*, **57**, 400–413.
- Brannigan, J. A. & Wilkinson, A. J. (2002). *Nature Rev. Mol. Cell Biol.* **3**, 964–970.
- Brooks, B. R., Bruccoleri, R. E., Olafson, B. D., States, D. J., Swaminathan, S., & Karplus, M. (1983). *J. Comp. Chem.* **4**, 187–217.
- Brooks, B. R., Janežič, D., & Karplus, M. (1995). *J. Comp. Chem.* **16**, 1522–1542.
- Buckle, A. M., Henrick, K., & Fersht, A. R. (1993). *J. Mol. Biol.* **234**, 847–860.

- Capriotti, E., Fariselli, P., & Casadio, R. (2005). *Nucleic Acids Res.* **22**, W306–W310.
- Carter, C. W., LeFebvre, B. C., Cammer, S. A., Tropsha, A., & Edgell, M. H. (2001). *J. Mol. Biol.* **311**, 625–638.
- Case, D. A. (1994). *Curr. Opin. Struct. Biol.* **4**, 285–290.
- Cheluvareja, S. & Meirovitch, H. (2005). *J. Chem. Phys.* **122**, 54903.
- Chiti, F., Stefani, M., Taddei, N., Ramponi, G., & Dobson, C. M. (2003). *Nature*, **424**, 805–808.
- Chiti, F., Taddei, N., Baroni, F., Capanni, C., Stefani, M., Ramponi, G., & Dobson, C. M. (2002). *Nature Struct. Biol.* **9**, 137–143.
- Chiti, F., Taddei, N., Bucciantini, M., White, P., Ramponi, G., & Dobson, C. M. (2000). *EMBO J.* **19**, 1441–1449.
- Cooper, A. (1976). *Proc. Natl. Acad. Sci. USA*, **73**, 2740–2741.
- de la Paz, M. L. & Serrano, L. (2004). *Proc. Natl. Acad. Sci. USA*, **101**, 87–92.
- Dobson, C. M. (2003). *Nature*, **426**, 884–890.
- Doig, A. J. & Sternberg, M. J. E. (1995). *Prot. Sci.* **4**, 2247–2251.
- DuBay, K. F., Pawar, A. P., Chiti, F., Zurdo, J., Dobson, C. M., & Vendruscolo, M. (2004). *J. Mol. Biol.* **341**, 1317–1326.
- Dunitz, J. D. (1995). *Chem. Biol.* **2**, 709–712.
- Efron, B. & Tibshirani, R. (1986). *Stat. Sci.* **1**, 54–75.
- Eisenmesser, E. Z., Bosco, D. A., Akke, M., & Kern, D. (2002). *Science*, **295**, 1520–1523.

- Eriksson, A. E., Baase, W. A., Zhang, X. J., Heinz, D. W., Blaber, M., Baldwin, E. P., & Matthews, B. W. (1992). *Science*, **255**, 178–183.
- Evans, P. A., Dobson, C. M., Kautz, R. A., Hatfull, G., & Fox, R. O. (1987). *Nature*, **329**, 266–268.
- Fersht, A. R., Matouschek, A., & Serrano, L. (1992). *J. Mol. Biol.* **224**, 771–782.
- Fieber, W., Kristjansdottir, S., & Poulsen, F. M. (2004). *J. Mol. Biol.* **339**, 1191–1199.
- Frauenfelder, H., Sligar, S. G., & Wolynes, P. G. (1991). *Science*, **254**, 1598–1603.
- Goehlert, V. A., Krupinska, E., Regan, L., & Stone, M. J. (2005). *Prot. Sci.* **13**, 3322–3330.
- Goodman, J. L., Pagel, M. D., & Stone, M. J. (2000). *J. Mol. Biol.* **295**, 963–978.
- Graur, D. & Li, W.-H. (2000). *Fundamentals of Molecular Evolution*. Sinauer Associates, 2nd edition.
- Gromiha, M. M., Uedaira, H., An, J., Selvaraj, S., Prabakaran, P., & Sarai, A. (2002). *Nucleic Acids Res.* **30**, 301–302.
- Guerois, R., Nielsen, J. E., & Serrano, L. (2002). *J. Mol. Biol.* **320**, 369–387.
- Henry, E. R. & Szabo, A. (1985). *J. Chem. Phys.* **82**, 4753–4761.
- Jorgensen, W. J., Chandrasekhar, J., Madura, J. D., Impey, R. W., & Klein, M. L. (1983). *J. Chem. Phys.* **79**, 926–935.
- Karplus, M. & Kushick, J. N. (1981). *Macromolecules*, **14**, 325–332.
- Karplus, M. & McCammon, J. A. (2002). *Nature Struct. Biol.* **9**, 646–652.

- Kay, L. E. (1998). *Nature Struct. Biol.* **5**, 513–517.
- Kay, L. E. (2005). *J. Magn. Reson.* **173**, 193–207.
- Klein-Seetharaman, J., Oikawa, M., Grimshaw, S. B., Wirmer, J., Durcharadt, E., Ueda, T., Imoto, T., Smith, L. J., Dobson, C. M., & Schwalbe, H. (2002). *Science*, **295**, 1719–1722.
- Kortemme, T. & Baker, D. (2002). *Proc. Natl. Acad. Sci. USA*, **99**, 14116–14121.
- Leatherbarrow, R. J. & Fersht, A. R. (1986). *Prot. Eng.* **1**, 7–16.
- Lee, A. L., Sharp, K. A., Kranz, J. K., Song, X.-J., & Wand, A. J. (2002). *Biochemistry*, **41**, 13814–13825.
- Levy, R. M., Karplus, M., Kushick, J., & Perahia, D. (1984). *Macromolecules*, **7**, 1370–1374.
- Li, Z., Raychaudhuri, S., & Wand, A. J. (1996). *Prot. Sci.* **5**, 2647–2650.
- Lindorff-Larsen, K. (2004). PhD thesis, University of Cambridge *Novel Approaches To Structure Determination of Denatured, Transition and Native States of Proteins*, Chapter 7, 91–100.
- Lindorff-Larsen, K., Best, R. B., DePristo, M. A., Dobson, C. M., & Vendruscolo, M. (2005). *Nature*, **433**, 128–132.
- Markley, J. L., Bax, A., Arata, Y., Hilbers, C. W., Kaptein, R., Sykes, B. D., Wright, P. E., & Wüthrich, K. (1998). *J. Mol. Biol.* **280**, 933–952.
- Matouschek, A., Kellis, J. T., Serrano, L., & Fersht, A. R. (1989). *Nature*, **340**, 122–126.
- Mayer, K. L., Earley, M. R., Gupta, S., Pichumani, K., Regan, L., & Stone, M. J. (2003). *Nature Struct. Biol.* **10**, 962–965.

- McCammon, J. A. & Wolynes, P. G. (1977). *J. Chem. Phys.* **66**, 1452–1456.
- McQuarrie, D. A. (2000). *Statistical Mechanics*. New York: Harper & Row.
- Millet, O., Mittermaier, A., Baker, D., & Kay, L. E. (2003). *J. Mol. Biol.* **329**, 551–563.
- Millet, O., Muhandiram, D. R., Skrynnikov, N. R., & Kay, L. E. (2002). *J. Am. Chem. Soc.* **124**, 6439–6448.
- Ming, D. & Brüschweiler, R. (2004). *J. Biomol. NMR*, **29**, 363–368.
- Mittermaier, A. & Kay, L. E. (2004). *Prot. Sci.* **13**, 1088–1099.
- Neria, E., Fischer, S., & Karplus, M. (1996). *J. Chem. Phys.* **105**, 1902–1921.
- Northey, J. G., Nardo, A. D., & Davidson, A. R. (2002). *Nature Struct. Biol.* **9**, 126–130.
- Paci, E. & Karplus, M. (1999). *J. Mol. Biol.* **288**, 441–459.
- Pawar, A. P., Dubay, K. F., Zurdo, J., Chiti, F., Vendruscolo, M., & Dobson, C. M. (2005). *J. Mol. Biol.* **350**, 379–392.
- Prompers, J. J. & Brüschweiler, R. (2000). *J. Phys. Chem. B*, **104**, 11416–11424.
- Qian, H. (1998). *J. Chem. Phys.* **109**, 10015–10017.
- Rasmussen, B. F., Stock, A. M., Ringe, D., & Petsko, G. A. (1992). *Nature*, **357**, 423–424.
- Ryckaert, J.-P., Ciccotti, G., & Berendsen, H. J. C. (1977). *J. Comput. Phys.* **23**, 327–341.
- Schwede, T., Kopp, J., Guex, N., & Peitsch, M. C. (2003). *Nucleic Acids Res.* **31**, 3381–3385.

- Serrano, L. & Fersht, A. R. (1989). *Nature*, **342**, 296–299.
- Serrano, L., Kellis, J. T. J., Cann, P., Matouschek, A., & Fersht, A. R. (1992). *J. Mol. Biol.* **224**, 783–804.
- Spyracopoulos, L. (2005). *Prot. Pep. Lett.* **12**, 235–240.
- Stone, M. J. (2001). *Acc. Chem. Res.* **34**, 379–388.
- Stone, M. J., Gupta, S., Snyder, N., & Regan, L. (2001). *J. Am. Chem. Soc.* **123**, 185–186.
- Vaughan, C. K., Buckle, A. M., & Fersht, A. R. (1999). *J. Mol. Biol.* **286**, 1487–1506.
- Wong, C. F. & McCammon, J. A. (2003). *Annu. Rev. Pharmacol. Toxicol.* **43**, 31–45.
- Wrabl, J. O., Shortle, D., & Woolf, T. B. (2000). *Proteins*, **38**, 123–133.
- Yang, D. & Kay, L. E. (1996). *J. Mol. Biol.* **263**, 369–382.
- Zhang, F. & Brüschweiler, R. (2002). *J. Am. Chem. Soc.* **124**, 12654–12655.
- Zhou, Y., Vitkup, D., & Karplus, M. (1999). *J. Mol. Biol.* **285**, 1371–1375.
- Zidek, L., Novotny, M. V., & Stone, M. J. (1999). *Nature Struct. Biol.* **6**, 1118–1121.

Captions

Fig. 1 Structural ensembles generated by restrained molecular dynamics simulations. Simulations were carried out for the wild-type (WT) Fyn SH3 domain, as well as two mutant forms (F20L and F20V), using S^2 values for amide and methyl mobilities as restraints (Best & Vendruscolo 2004).

Fig. 2 Back-calculation of S^2 values from structural ensembles generated by the restrained molecular dynamics approach. **A:** S^2 values for both amide and methyl groups were back-calculated and compared to the experimental values for the WT Fyn SH3 domain and its two mutational variants (F20L and F20V). **B:** Correlation between experimental and calculated changes in order parameters ($\Delta(S^2) = S^2_{mut} - S^2_{WT}$) for both the F20L and the F20V mutants of the Fyn SH3 domain.

Fig. 3 Distributions of side-chain χ dihedral angles (Markley *et al.* 1998) for 10 side-chains in the WT Fyn SH3 and its two mutational variants F20L and F20V. In each plot is shown the experimentally observed $\Delta(S^2) = S^2_{mut} - S^2_{WT}$ values for both F20L (blue) and F20V (red). The $\Delta(S^2)$ values shown for Leu29 and Val55 residues are the average values for the δ and γ methyl groups, respectively. The histograms show that the experimentally observed changes in S^2 values for methyl group mobility can be explained by relatively small variations in the distributions of side-chain dihedral angles.

Fig. 4 Estimating the entropic effects of the mutations using a quasi-harmonic analysis. **A:** Cumulative density of states for vibrational modes in WT, F20L and F20V Fyn SH3. The frequencies were obtained from a quasi-harmonic analysis (Brooks *et al.* 1995) of the structural ensembles as described in the methods section. The insert shows an expansion of the region between 0–2000 ns^{-1} . In the frequency range

larger than 2000 ns^{-1} the lines are essentially parallel meaning that the vibrational differences are found in the low frequency range. **B:** The configurational entropy was estimated from the vibrational frequencies and was used to calculate $T\Delta S_{vib}$ for the two mutations. The figure shows the results when different number of modes (starting from the low frequency end) are included in the calculations. Error bars correspond to one standard deviation and were estimated using a bootstrap procedure. The larger error bars obtained when including more than ≈ 250 modes in the analysis (corresponding to frequencies larger than $\approx 1000\text{ns}^{-1}$), is caused by the fact that bond lengths were kept approximately constant during the simulations (Ryckaert *et al.* 1977; Best & Vendruscolo 2004).

Figures

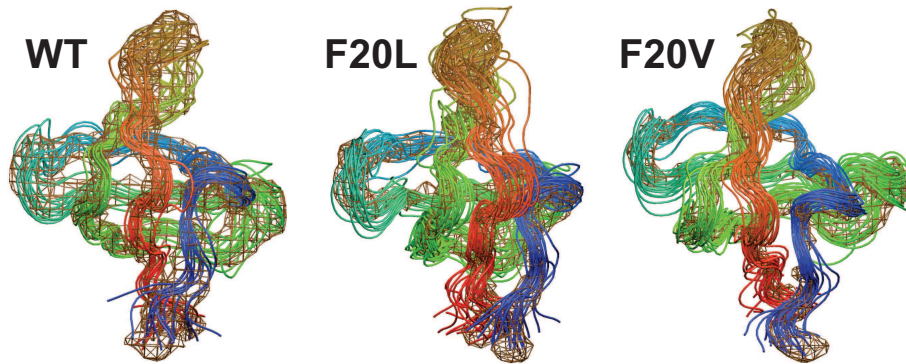


Figure 1:

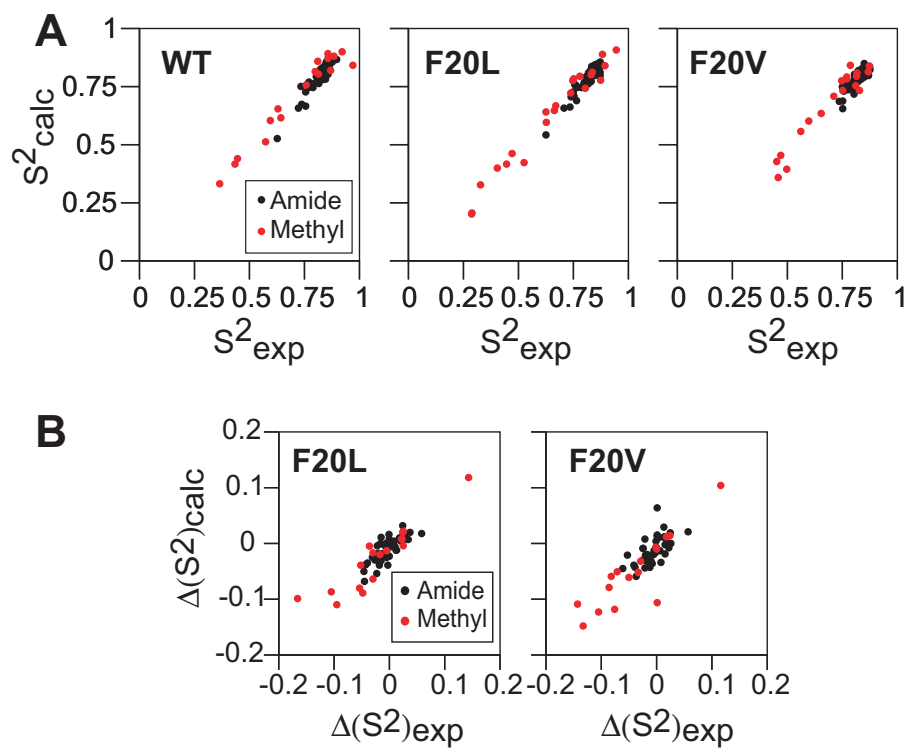


Figure 2:

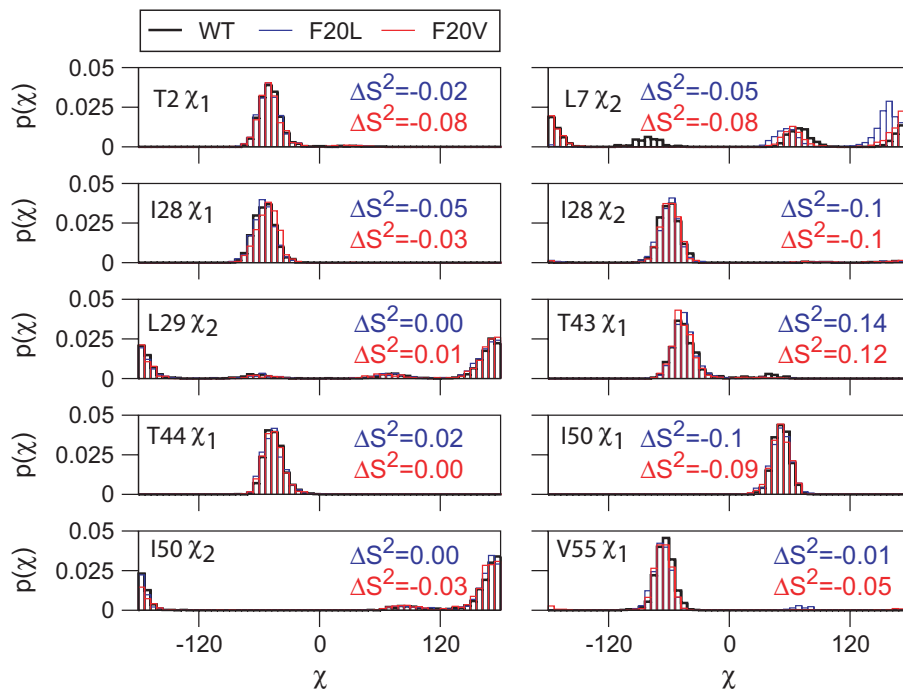


Figure 3:

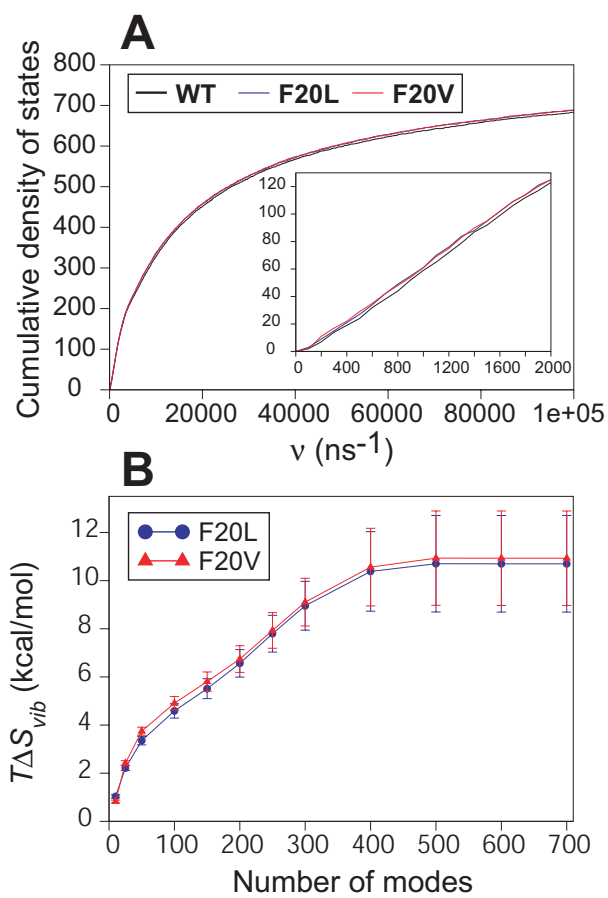


Figure 4: